7. Divgi CR, Larson SM. Radiolabeled monoclonal antibodies in the diagnosis and treatment of malignant melanoma. *Semin Nucl Med* 1989;29:252–261.
8. Michelot JM, Moreau MFC, Veyre AJ, et al. Phase II scintigraphic clinical trial of malignant melanoma and metastases with iodine-123-N-(2-diethylaminoethyl 4-iodobenzamide). *J Nucl Med* 1993;34:1260–1266.
9. Tonami N, Michigishi T, Bunko H, et al. Clinical tumor scanning with thallium-201-chloride. *Radioisotopes* 1976;25:67–69.
10. Mansi L, Salvadore M, DelVeccio S, et al. Imaging of melanoma with monoclonal F(ab'2) and thallium-201 chloride [Abstract]. *J Nucl Med* 1986;27:1022.
11. Rettenbacher L, Koller J, Galvan G. Detection of cutaneous metastatic melanoma with ^{201}Tl scintigraphy. *Clin Nucl Med* 1996;21:67.
12. Krasnow AZ, Collier BD, Isitman AT, et al. The clinical significance of unusual sites of thallium-201 uptake. *Semin Nucl Med* 1988;4:350–358.
13. Nadel HR. Thallium-201 for oncological imaging in children. *Semin Nucl Med* 1993;3:243–254.
14. Biersack HJ, Briele B, Hotze HL, et al. The role of nuclear medicine in oncology. *Ann Nucl Med* 1992;6:131–136.
15. Dadparvar S, Krishna L, Brady LW, et al. The role of iodine-131 and thallium imaging and serum thyroglobulin in the management of differentiated thyroid carcinoma. *Cancer* 1993;71:3767–3773.
16. Waxman AD, Ramanna L, Memsic LD, et al. Thallium scintigraphy in the evaluation of mass abnormalities of the breast. *J Nucl Med* 1993;34:18–23.
17. O'Tuama LA, Treves ST, Larar JN, et al. Thallium-201 versus technetium-99m-MIBI SPECT in evaluation of childhood brain tumors: a within-subject comparison. *J Nucl Med* 1993;34:1045–1051.
18. Mullins LJ, Moore RD. The movement of thallium ions in muscle. *J Gen Phys* 1960;43:759–773.
19. Sessler MJ, Geck P, Maul FD, Hör G, Munz DL. New aspects of cellular thallium uptake: Tl+-Na+-2C-l-cotransport is the central mechanism of ion uptake. *Nuklearmedizin* 1986;25:24–27.
20. Sehweil A, McKillop JH, Ziada G, et al. The optimum time for tumour imaging with thallium-201. *Eur J Nucl Med* 1988;13:527–529.
21. Sehweil AM, McKillop JH, Milroy R, et al. Mechanism of ^{201}Tl uptake in tumours. *Eur J Nucl Med* 1989;15:376–379.
22. Caluser C, Macapinlac H, Healey J, et al. The relationship between thallium uptake, blood flow, and blood pool activity in bone and soft tissue tumors. *Clin Nucl Med* 1991;17:565–572.
23. Ando A, Ando I, Katayama M, et al. Biodistributions of ^{201}Tl in tumor bearing animals and inflammatory lesion induced animals. *Eur J Nucl Med* 1987;12:567–572.
24. Ando A, Ando I, Katayama M, et al. Biodistributions of radioactive alkaline metals in tumor bearing animals: comparison with ^{201}Tl. *Eur J Nucl Med* 1988;14:352–357.
25. Maffioli L, Mascheroni L, Mongioj V, et al. Scintigraphic detection of melanoma metastases with a radiolabeled benzamide (iodine-123-(S)-IBZM). *J Nucl Med* 1994;35:1741–1747.
26. Blend MJ, Hyun H, Patel B, et al. Radioimmunoscintigraphy in patients with early stage cutaneous malignant melanoma. *J Nucl Med* 1996;37:252–257.
27. Morton DL, Wen DR, Cochran AJ. Management of early stage melanoma by intraoperative lymphatic mapping and selective lymphadenectomy. *Surg Oncol Clin North Am* 1992;1:247–259.

Technetium-99m-Tetrofosmin Uptake in Brain Tumors by SPECT: Comparison with Thallium-201 Imaging

Andrea Soricelli, Alberto Cuocolo, Andrea Varrone, Antonietta Discepolo, Enrico Tedeschi, Pier Paolo Mainenti, Maria Rosaria Grivet-Fojaja, Eugenio Maria Covelli, Alfredo Postiglione and Marco Salvatore

Department of Diagnostic Imaging, University of Naples Federico II, Nuclear Medicine Center of the National Research Council, and Department of Clinical and Experimental Medicine, University of Naples Federico II, Naples, Italy

Thallium-201 is clinically used for the assessment of primary and recurrent brain tumors. The biologic properties of ^{201}Tl that allow it to accumulate within the tumor cells render ^{201}Tl useful in evaluating tumor malignancy, but its physical characteristics and nonroutine availability limits its use in some institutions, as compared to ^{99m}Tc-labeled compounds. The aim of this study was to assess the feasibility of using ^{99m}Tc-tetrofosmin for imaging brain tumors and to compare its uptake with that of ^{201}Tl. **Methods:** Twenty-six patients with 27 intracranial masses were studied with SPECT. In the first group of seven patients (Group A), the timing for optimal acquisition of the ^{99m}Tc-tetrofosmin scan was assessed. In the second group of 19 patients (Group B), two sequential ^{201}Tl (74–148 MBq intravenous) and ^{99m}Tc-tetrofosmin (740–925 MBq intravenous) studies were performed 20 min after tracer injection and compared. **Results:** In Group A, no significant difference in the tumor-to-background (T/B) ratio among the 20-, 40- and 120-min postinjection studies was observed. In Group B, the quality of reconstructed images with ^{99m}Tc-tetrofosmin, judged visually, was superior to that of ^{201}Tl in 47% of all studies and was comparable in the remaining 53%. A significant relationship between ^{201}Tl and ^{99m}Tc-tetrofosmin T/B ratio ($r = 0.75$, $p < 0.01$) was found. The T/B ratio of ^{99m}Tc-tetrofosmin was significantly higher than that of ^{201}Tl (23.3 ± 21.5 compared to 6.1 ± 2.9, $p < 0.005$). **Conclusion:** Technetium-99m-tetrofosmin is a suitable radiotracer for the imaging of intracranial lesions with SPECT. Moreover, a better definition of tumor margins and a higher contrast between neoplastic and normal brain tissue can be achieved.

Received Jan. 16, 1997; revision accepted Aug. 6, 1997.

For correspondence or reprints contact: Andrea Soricelli, MD, Department of Diagnostic Imaging, University of Naples Federico II, Largo Torraca 71, 80133 Naples, Italy.

Key Words: brain imaging; technetium-99m-labeled compounds; intracranial lesions

J Nucl Med 1998; 39:802–806

Thallium-201 SPECT has been used successfully in the assessment of the biologic activity of primary and recurrent intracranial neoplasms due to its ability to accumulate within tumor cells (*1,2*). The metabolic state and growth rate of tumor cells are the most important factors determining ^{201}Tl uptake in vitro (*3,4*). In vivo, regional blood flow, blood-brain barrier (BBB) permeability and tissue viability are the main factors contributing to the uptake of the tracer (*5*). The increase in BBB permeability alone is not necessarily responsible for the uptake because some lesions, such as resolving hematomas and areas of radiation necrosis, show a low ^{201}Tl uptake (*6*). Tumor viability, on the other hand, is the most relevant factor responsible for ^{201}Tl uptake; in fact, a strict correlation of ^{201}Tl index, i.e., the tumor-to-background (T/B) ratio, with histologic grade, proliferative activity and overall prognosis of intracranial tumors has been demonstrated (*7*). Despite these considerable biologic advantages, ^{201}Tl has some limitations from the clinical standpoint. First, the long half-life and biologic distribution limit the amount of activity administered to the patient. Second, ^{201}Tl may be less available than ^{99m}Tc-labeled compounds in some institutions. Third, the low-energy photon flux of the radionuclide affects the quality of the image, particularly in brain tumors with diameters smaller than 1.5 cm, with a thin rim of ring enhancement during postcontrast magnetic resonance imaging (MRI) studies (*8*). However, optimal image quality with good definition of tumor size and margins is required for

TABLE 1
Technetium-99m-Tetrofosmin and Thallium-201 Tumor-to-Background Ratios in Group B Patients

Patient no.	Sex	Age (yr)	T/B ratio		Histology	Time to surgery* (day)	CT/MRI CE	Type of CE
			^{99m}Tc-tetrofosmin	^{201}Tl				
1	F	40	91.5	11.1	Hemangiopericitic meningioma	3	na	—
2	M	64	20.9	4.4	Metastasis (lung cancer)	12	Yes	Dysomogeneous
3	M	66	5.7	2.5	Metastasis (thyroid cancer)	30	Yes	Dysomogeneous
4	M	66	3.8	2.6	Transitional meningioma	30	Yes	Omogeneous
5	M	40	28.3	7.2	Endotheliomatous meningioma	14	Yes	Omogeneous
6	F	71	12.8	4.2	Angioblastic meningioma	1	Yes	Omogeneous
7	M	61	41.8	8.5	Transitional meningioma	10	Yes	Omogeneous
8	M	62	13.1	7.0	Metastasis (mesothelioma)	9	Yes	Omogeneous
9	M	56	16.8	3.9	Glioblastoma	7	Yes	Dysomogeneous
10	M	73	10.3	4.4	Recurrent angioblastic meningioma	10 yr before†	Yes	Omogeneous
11	M	61	31.1	8.7	Metastasis (parotid cancer)	12	Yes	Dysomogeneous
12	F	57	27.1	10.0	Hemangiopericitic meningioma	8	Yes	Omogeneous
13	F	58	13.9	3.8	High-grade oligodendroglioma	6	Yes	Dysomogeneous
14	F	62	21.7	9.6	Syncytial meningioma (recurrence)	5	Yes	Omogeneous
15	F	51	10.5	3.6	Metastasis (breast cancer)	No†	Yes	Omogeneous
16	F	60	Negative	Negative	Radiation necrosis	No†	No	—
17	M	19	Negative	Negative	Low-grade glioma	1	No	—
18	F	63	Negative	Negative	Giant carotid aneurysm	No†	Yes	Omogeneous
19	F	70	Negative	Negative	Arachnoid cyst	9	No	—
20	F	40	Negative	Negative	Colloid cyst III ventricle	4	No	—

*Time from SPECT imaging to neurosurgery.
†See Materials and Methods.
na = not available; CE = contrast enhancement.

the possibility of matching SPECT images with morphologic studies, such as CT and MRI.

Technetium-99m-labeled compounds are more suitable for SPECT imaging, and this raises the possibility of using such radiotracers for detecting brain neoplasms. Tetrofosmin (1,2-bis[bis(2-ethoxyethyl)phosphino]ethane) is a new agent that, with ^{99m}Tc, forms a lipophilic cationic complex and is used in clinical practice for the evaluation of myocardial perfusion (*9*). This compound seems to localize within mitochondria, and the biodistribution models have shown a good heart uptake with rapid blood, lung and liver clearance and very low retention at the level of the brain tissue (*10,11*).

The aims of this study were:

1. To assess the ability of ^{99m}Tc-tetrofosmin to detect intracranial neoplasms in a group of patients with a previous positive ^{201}Tl scan;
2. To determine the best imaging time after the injection; and
3. To correlate ^{201}Tl and ^{99m}Tc-tetrofosmin uptake in a second group of patients with heterogeneous intracranial masses.

MATERIALS AND METHODS

Patient Inclusion

In this study, of the patients referred to the Diagnostic Imaging Department of the University Federico II of Naples with MRI and/or CT evidence of intracranial mass, those who underwent both ^{201}Tl and ^{99m}Tc-tetrofosmin SPECT scans were included. Patients were under standard antiedema or antiepileptic drugs whenever required. All patients gave informed consent to participate to the study. Histologic diagnosis was obtained for all except five patients. One patient (Patient 10, Table 1) had undergone surgery 10 yr before the SPECT study for an angioblastic meningioma and had not undergone any subsequent surgery. Another patient (Patient 15, Table 1) also had a bone metastasis from a breast cancer localized at the level of a dorsal vertebra; both brain and bone lesions were treated with radiotherapy. The third patient's (Patient 16, Table 1), MRI scan showed a large left fronto-parietal area of low signal on T1-weighted images and of high signal on DP- and T2-weighted images with no contrast enhancement, which was interpreted as an area of radiation necrosis and was confirmed during clinical follow-up. The fourth patient (Patient 18, Table 1) showed a right parasellar lesion with omogeneous contrast enhancement at the CT scan that was initially interpreted as a cavernous sinus meningioma; afterward, the patient underwent digitalized carotid angiography, which showed the presence of a giant carotid aneurysm. An extra cranial-intra cranial (EC-IC) bypass was programmed to perform an endovascular treatment of the aneurysm.

Another patient (Patient 1, Table 2) had undergone surgery 2 yr before the SPECT study for a metastasis from a breast cancer; at the time of the study, the patient presented with a recurrence of the brain tumor and died 7 days after the SPECT study. Surgery was not performed in this patient due to her poor clinical condition.

All other patients underwent surgery 9.1 ± 8.1 days (range 1–30 days) after the SPECT study (Tables 1 and 2). In these patients, the SPECT studies were performed in adjunct to the CT and MRI studies for the functional assessment of intracranial neoplasms. In each case, the decision regarding the resulting treatment was made with consideration of the results of both anatomical and functional studies.

CT, MRI and Magnetic Resonance-SPECT Fusion Images

CT studies were performed in 20 patients with a Siemens Somatom HIQ unit (Siemens, Erlangen, Germany), whereas MRI studies were performed in 11 patients using a 1.5-Tesla Magnetom SP 63 (Siemens). Transaxial, sagittal and coronal slices were obtained using multiple sequences, yielding T1-, DP- and T2-weighted MR images. For CT and MRI contrast enhancement studies, patients received either 100 ml of non-ionic contrast medium or 0.1 mmol/kg Gd-DTPA intravenously.

Images of anatomical and functional correlation (fusion images) were obtained by averaging the grayscale T1 MR image with the

TABLE 2
Tumor-to-Background Ratios of Technetium-99m-Tetrofosmin at 20, 40 and 120 Minutes (First, Second and Third Scan, Respectively) Postinjection in Group A Patients

Patient no.	Sex	Age (yr)	T/B ratio 1st scan	T/B ratio 2nd scan	T/B ratio 3rd scan	Histology	Time to surgery* (day)	CT/MRI CE	Type of CE
1	F	54	23.0	25.3	21.9	Recurrence of breast cancer metastasis	2 yr before†	Yes	Dysomogeneous
2	F	41	28.5	20.8	16.9	Transitional meningioma	3	Yes	Omogeneous
3	F	45	17.5	18.1	9.0	Oligodendroglioma (recurrence)	2	Yes	—
4	F	68	32.2	34.7	17.1	Syncytial meningioma	12	na	—
5	M	47	31.6	31.8	—	Metastasis (pulmonary carcinoid)	5	Yes	Dysomogeneous
6	M	56	16.8	18.4	—	Glioblastoma	7	Yes	Dysomogeneous
7	M	62	13.1	7.5	—	Metastasis (mesothelioma)	9	Yes	Omogeneous

*Time from SPECT imaging to neurosurgery.
†See Materials and Methods.
na = not available; CE = contrast enhancement.

red, green and blue components of the corresponding color scale SPECT image after appropriate windowing.

Preliminary Study

The first group (Group A) included seven patients (3 men, 4 women; mean age = 53.3 ± 9.7 yr; age range 41–68 yr) with the following lesions: three metastases, two meningiomas, one recurrent oligodendroglioma and one glioblastoma (Table 2). All patients were studied with two SPECT acquisitions of 15 min each, starting at 20 and 40 min after intravenous injection of 740 MBq ^{99m}Tc-tetrofosmin (Myoview Amersham, Bucks, United Kingdom). In four of these patients, a subsequent 15-min scan at 120 min after injection was also performed. All scans were acquired with a matrix of 128 × 128 × 64, using a high-resolution, brain-dedicated SPECT device (Ceraspect; DSI, Waltham, MA).

The images were reconstructed using a two-dimensional Butterworth filter (cutoff = 0.90 cm, order 10) and attenuated with the Chang algorithm, obtaining 64 1.67-mm-thick transaxial slices. These slices were summed in groups of 6 to obtain 11 9.6-mm-thick slices. For semiquantitative analysis of the T/B ratio, two asymmetric regions of interest (ROIs) were drawn. One elliptical ROI was positioned on the tumor site (tumor ROI), at the brain level which showed the best evidence of the lesion. The background ROI was manually drawn encompassing the whole contralateral normal brain hemisphere within the scalp, excluding the choroid plexus. The ratio was calculated as the mean counts per pixel in the tumor ROI/mean counts per pixel in the background ROI (T/B ratio). Because data analysis was performed on a ratio between mean counts/pixel, no decay correction was applied.

Comparative Study

The second group (Group B) included 19 patients (9 men, 10 women; mean age = 56.6 ± 13.4 yr; age range 19–73 yr) with 20 intracranial lesions: 5 metastases, 8 meningiomas, 1 low-grade glioma, 1 high-grade glioma, 1 glioblastoma, 1 giant carotid aneurysm, 1 arachnoid cyst, 1 colloid cyst of III ventricle and 1 case of radiation necrosis (Table 1). In this group, a 20-min ^{201}Tl-SPECT scan was performed, starting 20 min after the intravenous injection of 74–148 MBq ^{201}Tl-chloride (Mallinckrodt, Inc., B.V. Petten, the Netherlands). The images were acquired with a 128 × 128 × 64 matrix, reconstructed using a two-dimensional Butterworth filter (cutoff = 1.00 cm, order 10) and attenuated in the same way as in the ^{99m}Tc-tetrofosmin study. At the end of ^{201}Tl acquisition, without moving the patient, 740–925 MBq of ^{99m}Tc-tetrofosmin were intravenously injected. Starting 20 min after the injection, a 15-min SPECT scan was then performed.

A visual analysis of image quality for ^{201}Tl and ^{99m}Tc-tetrofosmin studies (assessed on the basis of the contrast of the lesion to the background and the definition of tumor's margins) was performed by two experienced observers who had no knowledge of the radiopharmaceutical, clinical status and CT or MRI findings. The visualization of the interfering activity of the choroid plexus was also considered in the visual analysis of the images.

Semiquantitative data analysis was performed, for both tracers, with the same method described previously for the preliminary study.

Statistical Analysis

Data are reported as mean ± s.d. The relationship between the ^{99m}Tc-tetrofosmin and ^{201}Tl T/B ratio was assessed with the Pearson coefficient (r) and plotted with a linear regression equation. Technetium-99m-tetrofosmin and ^{201}Tl T/B ratio were compared using paired Student's t-test. A p value of less than 0.05 was considered statistically significant.

RESULTS

Pattern of Contrast Enhancement on CT and MRI

The patterns of contrast enhancement for CT and MRI studies are reported in Tables 1 and 2 for both groups of patients. The type of contrast enhancement was classified as omogeneous or dysomogeneous, on the basis of the distribution of the contrast material within each lesion.

Preliminary Study

In all seven patients of Group A (Table 2), high tracer uptake in the tumor site was already clearly evident in the 20-min ^{99m}Tc-tetrofosmin scan. The semiquantitative analysis showed a mean value for the ^{99m}Tc-tetrofosmin T/B ratio of 23.3 ± 7.7 in the 20-min scan and of 22.4 ± 9.2 in the 40-min scan (p = not significant).

In patients undergoing a scan 120-min after intravenous tracer injection, the mean value for the ^{99m}Tc-tetrofosmin T/B ratio was 16.3 ± 5.3. The T/B ratio at 120 min was lower than that of the previous scans, and in two patients (Patients 3 and 4, Table 2), it was about two-fold lower. However, the mean value for ^{99m}Tc-tetrofosmin T/B ratio was not significantly different compared to both the 20- and 40-min scans.

Because the T/B ratio of the 20-min scan was not significantly different from that of the 40- and 120-min scans, the earlier scan was chosen for imaging intracranial masses with ^{99m}Tc-tetrofosmin SPECT so that patients would be in a more comfortable position. Figure 1 shows the ^{99m}Tc-tetrofosmin SPECT at three different imaging times in Patient 3 of Group A, who had a recurrent oligodendroglioma.

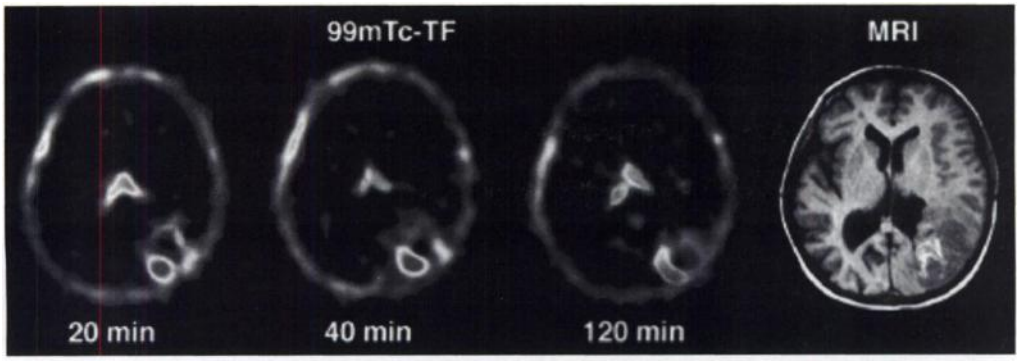

FIGURE 1. Technetium-99m-tetrofosmin images at three different times and a MRI at the same level in a patient who had a recurrence of oligodendroglioma (Patient 3 of Group A, Table 2).

Comparative Study

During visual analysis, ^{99m}Tc-tetrofosmin tomograms in four of the five patients with metastatic lesions and in two of the three patients with high-grade intracranial neoplasms were judged to be superior in quality to ^{201}Tl tomograms. In one of the patients with glioblastoma (Patient 9 of Group B, Table 1), although a clearer definition of the tumor's margins was observed with ^{99m}Tc-tetrofosmin, the activity of the choroid plexus partially interfered with the visualization of the tumor. In six of seven patients with meningioma, ^{99m}Tc-tetrofosmin and ^{201}Tl images were judged to be of comparable quality. In one patient with transitional meningioma (Patient 4 of Group B, Table 1), the ^{99m}Tc-tetrofosmin image was judged to be superior in quality to the ^{201}Tl image.

Five lesions (Patients 16–20, Table 1) showed no uptake with either tracer and, therefore, were not included in the semiquantitative analysis. A statistically significant relationship between ^{201}Tl and ^{99m}Tc-tetrofosmin T/B ratio was observed ($r = 0.75$, $p < 0.01$) (Fig. 2). The mean value of T/B ratio for the ^{99m}Tc-tetrofosmin study (23.3 ± 21.5) was significantly higher ($p < 0.005$) than that of ^{201}Tl (6.1 ± 2.9). Figure 3 shows the uptake of the two tracers in a patient with a metastasis of a parotid cancer (Patient 11, Table 1).

DISCUSSION

The main finding of this study is the suitability of ^{99m}Tc-tetrofosmin as a potential radiotracer for the imaging of intracranial lesions. Moreover, the 20-min ^{99m}Tc-tetrofosmin SPECT scan provides a better depiction of the tumor mass than the ^{201}Tl scan, with lower background activity.

Thallium-201 and ^{99m}Tc-tetrofosmin showed a similar accumulation pattern in the brain because both tracers were almost completely excluded from normal cerebral tissue, and their distribution within the whole lesion was substantially equivalent. The only differences between the two tracers were the consistent and high uptake of ^{99m}Tc-tetrofosmin by the normal choroid plexus and the scalp and the very low background of tracer uptake compared with that of ^{201}Tl. Therefore, ^{99m}Tc-tetrofosmin may be limited in the evaluation of lesions lying close to the ventricles, but it otherwise allows better visualization of the tumor's margins. The ability to better visualize tumor margins could also be considered an advantage in imaging tumors lying deeply in the brain because, in these cases, even the ^{201}Tl findings could be limited by tracer accumulation in the regions of the plexus (*12*).

Mechanism of Technetium-99m-Tetrofosmin Uptake

The mechanism of ^{99m}Tc-tetrofosmin uptake has been studied in myocardial cells, and it seems to be dependent on cellular metabolism (*13*) because mitochondria take up the tracer with a process that is dependent on their membrane potential and coupling state (i.e., their ability to couple oxidative phosphorylation) (*14*). In our series of patients, ^{99m}Tc-tetrofosmin was completely excluded by the normal brain tissue, so the breakdown or an increased permeability of the BBB seems to be a

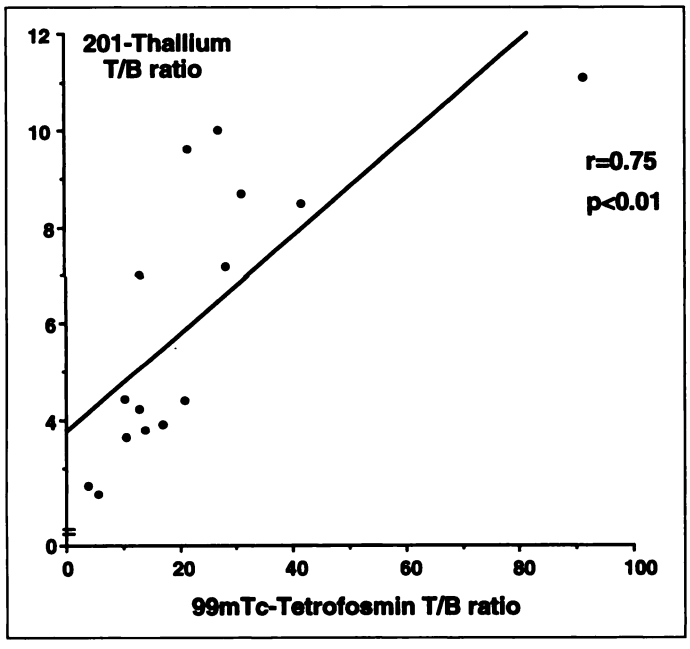

FIGURE 2. Relationship between ^{201}Tl and ^{99m}Tc-tetrofosmin T/B ratio in Group B patients.

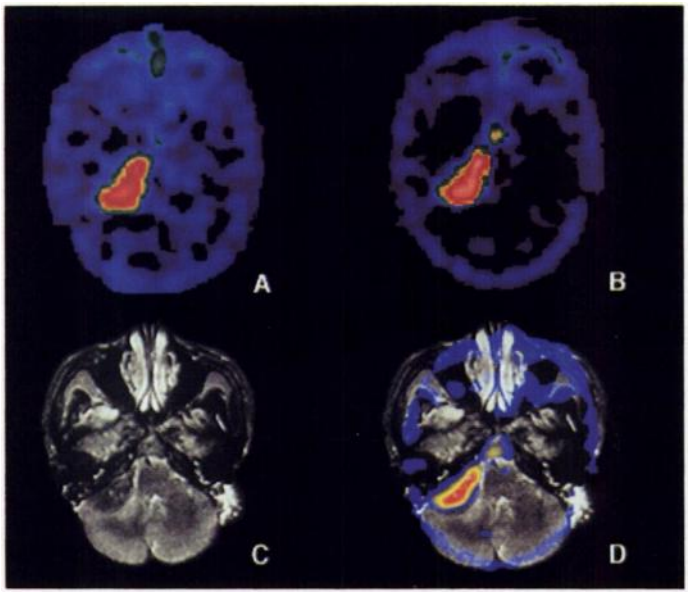

FIGURE 3. Thallium-201 (A), ^{99m}Tc-tetrofosmin (B), MR (C) and fusion (D) images in a patient with a metastasis of a parotid cancer (Patient 11 of Group B, Table 1). The lesion shows high uptake of both tracers.

condition necessary for tracer uptake by the tumor. Nevertheless, in a tumor cell line, it has been shown that the uptake mechanism, intracellular distribution and washout kinetics of ^{99m}Tc-tetrofosmin are influenced by compounds that interfere with metabolic processes (*15*) and that the mechanisms by which the tracer enters the cells depend on both cell membrane (Na^+/K^+ pump) and mithocondrial potentials (*16*).

Thus, the uptake of ^{99m}Tc-tetrofosmin seems to be related to tissue viability, and in our study, it can be assumed that the presence of viable tissue is an important factor responsible for the tracer retention. However, although no significant difference was found in the T/B ratio at three different times from the injection, the T/B ratio tended to decrease in the later scan, and in two patients, it was about two-fold lower than the initial scan. In the patient with a syncytial meningioma, the marked decrease of the T/B ratio at 2 hr might have been related to the prevalent vascularity of the lesion, as compared to the cellular component, which could have influenced the rate of the tracer washout from the tumor. In the other patient (Fig. 1), an area of the tumor showed a dysomogeneous gadolinium contrast enhancement and a time-invariant uptake over a 2-hr interval. This might indicate that the tracer distribution was not xomogeneous in the whole lesion, with at least one area showing a more pronounced altered BBB permeability, with a clear tendency to retain the tracer, probably due to an increased cellularity.

We could not assess which of these two factors, i.e., BBB permeability or tissue viability, was mainly responsible for the ^{99m}Tc-tetrofosmin uptake because we did not study enough lesions at different times to draw substantial conclusions, but it is well known that, even for thallium uptake, brain lesions present different washout kinetics on the basis of the histologic grade (*17*). In fact, it has been demonstrated that the time-dependent change in the thallium index is related to the vascularity and presence of viable tissue within brain tumors (*8,17,18*). In our work, the kinetic behavior of ^{99m}Tc-tetrofosmin was not extensively evaluated because the main point of this study to assess this tracer's ability to image intracranial lesions compared to a standard tracer such as thallium.

Comparison of Thallium-201 and Technetium-99m-Tetrofosmin

Despite different mechanisms of uptake, the accumulation of both tracers was similar in all the tumors studied. Only one low-grade glioma (Patient 17 of Group B) could not be detected by either ^{99m}Tc-tetrofosmin or ^{201}Tl, whereas in all the remaining patients, the tumor was clearly revealed by both tracers. The two tracers showed a significant correlation in the ability to detect brain tumors, but it was found that the average ^{99m}Tc-tetrofosmin T/B ratio was significantly higher than that of ^{201}Tl in the whole group and that all individual lesions showed higher ^{99m}Tc-tetrofosmin T/B ratios (Table 1). This difference is likely due to lower background activity in the ^{99m}Tc-tetrofosmin studies compared to that of ^{201}Tl. No direct comparison was made between the background value of the two radiotracers because of their difference in the physical properties. Nevertheless, different kinetics of the two tracers might have influenced the T/B ratio at a specific acquisition time. However, because no statistical difference was found in the T/B ratio of ^{99m}Tc-tetrofosmin at the three different times, it was concluded that these findings were due to an actual difference in the distribution of the tracers in neoplastic and non-neoplastic tissue, with ^{99m}Tc-tetrofosmin being more completely excluded by normal tissue than ^{201}Tl. The main outcome of this finding is the better image quality obtained with ^{99m}Tc-tetrofosmin in several different intracranial masses. In fact, the quality of tumor images, despite the limitation of choroid plexus uptake, was better with ^{99m}Tc-tetrofosmin because the margins of the lesions and the boundaries between nonpathologic and pathologic tissue were easily detected. Some ^{201}Tl uptake also occurred in the region of the choroid plexus but less distinctly than with ^{99m}Tc-tetrofosmin. In addition, ^{99m}Tc-tetrofosmin is a ^{99m}Tc-labeled compound, with considerable practical advantages compared with ^{201}Tl (i.e., optimal photopeak energy, higher administered activity with less radiation dose to the patient and easy availability). Finally, no attempt was made to assess the grading of gliomas with ^{99m}Tc-tetrofosmin because of the limited number of such lesions studied. Further studies with a larger number of patients are required to assess the possibility of achieving functional characterization of primary and recurrent brain tumors with ^{99m}Tc-tetrofosmin and SPECT.

CONCLUSION

This study presents preliminary data on the comparison between ^{99m}Tc-tetrofosmin and ^{201}Tl imaging of brain tumors and shows that functional imaging of intracranial lesions may be performed with ^{99m}Tc-tetrofosmin SPECT, which has some advantages over ^{201}Tl, mainly, a better definition of tumor margins and higher contrast between tumor and normal brain tissue.

ACKNOWLEDGMENTS

This study was partially supported by the "Associazione Italiana per la Ricerca sul Cancro."

REFERENCES

1. Kaplan WD, Takvorian T, Morris JH, Rumbaugh CL, Connolly BT, Atkins HL. Thallium-201 brain tumor imaging: a comparative study with pathologic correlation. *J Nucl Med* 1987;28:47–52.
2. Kim KT, Black KL, Marciano D, et al. Thallium-201 SPECT imaging of brain tumors: methods and results. *J Nucl Med* 1990;31:965–969.
3. Elligsen JD, Thompson JE, Frey HE, Kruvv J. Correlation of (Na+-K+)ATPase activity with growth of normal and transformed cells. *Exp Cell Res* 1974;87:233–240.
4. Kasarov LB, Friedmann H. Enhanced Na+-K+ activated adenosine triphosphatase activity in transformed fibroblasts. *Cancer Res* 1974;34:1862–1865.
5. Atkins HL, Budinger TF, Labowitz E, et al. Thallium-201 for medical use. Part 3: human distribution and physical imaging properties. *J Nucl Med* 1977;18:133–140.
6. Black KL, Hawkins RA, Kim KT, Becker DP, Lerner C, Marciano D. Use of thallium-201 SPECT to quantitate malignancy grade of gliomas. *J Neurosurg* 1989; 71:342–346.
7. Oriuchi N, Tamura M, Shibazaki T, et al. Clinical evaluation of thallium-201 SPECT in supratentorial gliomas: relationship to histologic grade prognosis and proliferative activities. *J Nucl Med* 1993;34:2085–2089.
8. Yoshii Y, Satou M, Yamamoto T, et al. The role of thallium-201 single photon emission tomography in the investigation and characterisation of brain tumours in man and their response to treatment. *Eur J Nucl Med* 1993;20:39–45.
9. Cuocolo A, Soricelli A, Nicolai E, et al. Technetium-99m-tetrofosmin regional myocardial uptake at rest: relation to severity of coronary stenosis in previous myocardial infarction. *J Nucl Med* 1995;36:907–913.
10. Kelly JD, Forster AM, Higley B, et al. Technetium-99m-tetrofosmin as a new radiopharmaceutical for myocardial perfusion imaging. *J Nucl Med* 1993;34:222–227.
11. Jones S, Hendel RC. Technetium-99m tetrofosmin: a new myocardial perfusion agent. *J Nucl Med Technol* 1993;21:191–195.
12. O'Tuama LA, Janicek M, Barnes PD, et al. Thallium-201/^{99m}Tc-HMPAO SPECT imaging of treated childhood brain tumors. *Pediatr Neurol* 1991;11:249–257.
13. Platts EA, North TL, Pickett RD, Kelly JD. Mechanism of uptake of technetium-tetrofosmin. I: uptake into isolated adult rat ventricular myocytes and subcellular localization. *J Nucl Cardiol* 1995;2:317–326.
14. Younès A, Songadele JA, Maublant J, Platts E, Pickett R, Veyre A. Mechanism of uptake of technetium-tetrofosmin. II: uptake into isolated adult rat heart mitochondria. *J Nucl Cardiol* 1995;2:327–333.
15. Arbab AS, Koizumi K, Toyama K, Arai T, Araki T. Uptake of ^{99m}Tc-tetrofosmin in a tumor cell line: comparison with ^{99m}Tc-MIBI [Abstract]. *J Nucl Med* 1996;37 (suppl):254P.
16. Arbab AS, Koizumi K, Toyama K, Araki T. Uptake of technetium-99m-tetrofosmin, technetium-99m-MIBI and thallium-201 in a tumor cell lines. *J Nucl Med* 1996;37: 1551–1556.
17. Ueda T, Kaji Y, Wakisaka K, et al. Time sequential single photon emission computed tomography studies in brain tumour using thallium-201. *Eur J Nucl Med* 1993;20: 138–145.
18. Moustafa HM, Omar WM, Ezzat I, Ziada GA, El-Ghonimy EG. Thallium-201 single photon emission tomography in the evaluation of residual and recurrent astrocytoma. *Nucl Med Commun* 1994;15:140–143.